IEEE Access
Multidisciplinary | Rapid Review | Open Access Journal

Received January 8, 2022, accepted February 9, 2022, date of publication February 11, 2022, date of current version February 18, 2022.

Digital Object Identifier 10.1109/ACCESS.2022.3151104

Impact of Surfactants on the Electrical and Rheological Aspects of Silica Based Synthetic Ester Nanofluids

S. K. AMIZHTAN[1], A. J. AMALANATHAN[1], R. SARATHI[1], (Senior Member, IEEE), BALAJI SRINIVASAN[1], (Member, IEEE), RAMESH L. GARDAS[2], HANS EDIN[3], (Member, IEEE), AND NATHANIEL TAYLOR[3], (Member, IEEE)

[1]Department of Electrical Engineering, Indian Institute of Technology Madras, Chennai 600036, India
[2]Department of Chemistry, Indian Institute of Technology Madras, Chennai 600036, India
[3]School of Electrical Engineering and Computer Science, KTH-Royal Institute of Technology, 10044 Stockholm, Sweden

Corresponding author: R. Sarathi (rsarathi@iitm.ac.in)

This work was supported by the Department of Science and Technology (DST) through Nano Mission on Transformer Insulation, New Delhi, India, under Grant DST/NM/NT/2018/33 (C) & (G).

ABSTRACT This study reports experimental investigations of the effects of different surfactants (CTAB, Oleic acid and Span 80) on silica based synthetic ester nanofluids. The positive and negative potential observed for the ionic (CTAB) and non-ionic surfactant (Span 80) from zeta potential analysis indicates an improved stability. The optimization of nanofillers and surfactants is performed considering the corona inception voltage measured using ultra high frequency (UHF) technique and fluorescent fiber. Rheological analysis shows no significant variation of properties with shear rate, implying Newtonian behavior even with the addition of surfactant. In addition, the permittivity of the nanofluid is not much affected by adding surfactant but a marginal variation is noticed in the loss tangent with the effect of temperature. The fluorescence spectroscopy shows no change in the emission wavelength with the addition of silica nanofiller and surfactants. Flow electrification studies indicate an increase in the streaming current with the rotation speed and temperature, with a higher current magnitude observed in the case of nanofluids.

INDEX TERMS Synthetic ester, silica, stability, fluorescence, shear rate, viscosity, loss tangent, streaming current.

I. INTRODUCTION

Oil filled power transformers form an important part of the power system network. Their insulation design is critical for long and reliable operation. Mineral oils have long been used as an insulant and coolant. Their low degradability level and environmentally toxic nature have led to much research on finding alternative fluids for transformers, that are now being tested. Recently, ester-based fluids have gained importance because of their higher fire class properties and excellent biodegradability compared to mineral oil [1], [2]. There is also need to design and develop suitable insulating structures for transformers with better dielectric properties due to increased voltage levels of operation, space constraints and other economic concerns. One possible step towards this requirement is to disperse suitable insulative and semi-conductive nanoparticles into the liquid insulation [3]. In the recent times, considerable research has been carried out on synthetic esters to improve electrical and thermal characteristics of insulant by the inclusion of different nanoparticles [4]–[6]. In the present study, the performance of silica (SiO_2) nanoparticles was investigated because of its increased breakdown voltage and excellent dielectric properties [7], [8]. However, it remains difficult to determine an optimal quantity of nanofiller, in this case SiO_2 nanoparticles, to achieve optimum breakdown strength, which is one of the major objectives of this work.

The nanofillers in the insulating liquid must have uniform dispersion and stability, and many methods for preparing nanofluids have been employed in research and practice, with the two-step procedure being the most extensively utilized. Because of the attraction force existing between nearby particles, nanoparticles dispersed in the base fluid form clusters leading to agglomeration, thereby resulting in decreased

The associate editor coordinating the review of this manuscript and approving it for publication was Guillaume Parent.

surface energy. The presence of surface charges on scattered particles gives rise to the ionic characteristics where the Stern layer is formed when opposite charges adhere to the surface of scattered particles, generating a layer of charged ions, and a slipping plane around this ridged layer. The potential difference between the dispersion medium and the sliding plane is known as the zeta potential and its magnitude gives an indication of the stability of the prepared nanofluids, which are considered to be stable only if the zeta potential is above ±30 mV [9]. Methods that are used to improve the stability include changing the pH, chemically altering the fluid, and adding surfactants [10]. The use of a surfactant is an important aspect of the second stage since it provides a simple and cost-effective way to improve the nanofluid's stability. In addition, the surfactant also influences the interfacial region between particle and the fluid, forming a stable composite mixture. The surfactants such as cetyl trimethyl ammonium bromide (CTAB), sodium dodecyl benzene sulfonate (SDBS), oleic acid and Span-80 involving both ionic and non-ionic structures are used for improving the stability of nanofluids [11], [12].

The occurrence of corona owing to protrusion from the winding conductor is the leading causes of transformer insulation failure [13] and the identification of such incipient discharges is a difficult task, where several techniques such as phase acoustic emission technique, dissolved gas analysis and radio frequency (RF) methodology are used for its detection at an early stage [14]. The injected current pulse caused by partial discharges in transformer oil has a rising period of a few nanoseconds, which excites electromagnetic signals in the range of 300-3000 MHz, the ultra-high frequency (UHF) range. There have been various literatures involved on the usage of UHF technique [15] for the detection of partial discharges (PD). Fluorescent fiber detection methods are becoming increasingly popular and their properties for detecting PD activity have to be clearly understood. Another major phenomenon that occurs in large power transformers is static electrification, which occurs when the circulating oils used for heat dissipation from the windings induce surface charge accumulation on the solid insulation, and can lead to complete flashover of pressboard spacers over a longer period of time [16]. Hence, it is required to understand the streaming phenomenon of nanofluids at the pressboard interfaces as not much data is available in the literature. The spinning disc approach uses a small volume of insulating fluid, and creates an electrical double layer at the fluid/pressboard interface, controlled by centrifugal force. Mineral oil and ester-based fluids used in transformers are Newtonian fluids with an electrical double layer development that differs from that of non-Newtonian fluids. Also, the effect of several characteristics on the streaming current, such as viscosity, conductivity, and shear rate, has been examined [17]. It is therefore critical to investigate the rheological pattern of insulating fluids in order to investigate the production of streaming currents in which the fluid's visco-elastic characteristics are altered by stress and strain.

The following methodological experimental studies were carried out to understand the impact of surfactant on properties of nano silica ester fluid (i) stability of nanofluid using zeta potential measurement, (ii) rheological aspects of nanofluids, (iii) variation in corona inception voltage due to surfactant in nano fluids under AC and DC voltages, using fluorescence and UHF measurement techniques, (iv) variation in fluorescent properties of ester nanofluid due to surfactant, (v) variation in permittivity and loss tangent with different surfactant in nano fluid, and (vi) fluorescence spectroscopy and flow electrification phenomenon with the influence of temperature.

II. EXPERIMENTAL PROCEDURE

A. PREPARATION OF NANOFLUIDS

Synthetic ester (MIDEL 7131) was used as the base fluid throughout this work. Silica nanoparticles were procured from Nanostructured and Amorphous Materials Inc., with a mean particle size of 15 nm. Different surfactants such as CTAB, Oleic acid and Span-80 were studied for their effect on the stability of silica nanofillers in ester fluid. The process for nanofluid sample preparation is shown in Fig. 1. The silica nanoparticles were heated at 150°C for 8 hours to remove moisture content. Initially, the surfactant was mixed with synthetic ester fluid using a magnetic stirrer for 30 minutes and then the silica nanoparticles were added to the mixture, which then had magnetic stirring again to hold the nanoparticles on the surfactant chain. Finally, the colloidal mixture was fed to the ultra-sonification process (Sonic Vibra cell sonicator) at 20 kHz for 3 hours. The prepared nanofluids were then placed in a vacuum desiccator for removal of gas bubbles. This was followed by a resting time period before performing the experiments, in order to confirm stable dispersion of nanoparticles. The sample compositions of prepared nanofluids used in this work are shown in Table 1.

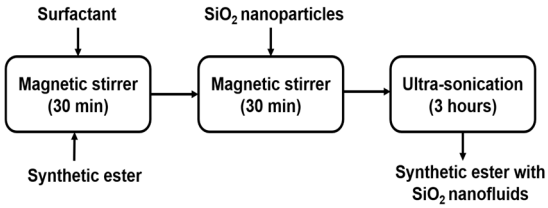

FIGURE 1. Setup for corona inception voltage test.

TABLE 1. Sample composition used for test and analysis.

Base fluid	Nanoparticle	Surfactant	Sample
Synthetic Ester	-	-	A
Synthetic Ester	Silica	-	B
Synthetic Ester	Silica	CTAB	C
Synthetic Ester	Silica	Oleic acid	D
Synthetic Ester	Silica	Span-80	E

B. HIGH VOLTAGE SOURCE AND SENSOR

The experimental setup used for corona inception voltage (CIV) measurement is shown in Fig. 2. High voltage is generated by a Trek amplifier (Model 20/20C) controlled from a function generator. The test cell has a point-plane electrode setup with a 0.5 mm electrode tip and a 50 mm ground electrode. A fluorescent fibre and a silicon photomultiplier (SiPM) module are used in the fluorescence approach for corona detection. The fibre is a Saint Gobain crystals BCF 91A green fibre, of length 1 m and diameter 1 mm. One end of the fibre is placed into the SiPM module (SensL's MicroFC SMA 10050) and the other end is looped around the test cell near the needle tip. The unexposed part of the fibre is shielded with a fibre sleeve to reduce signals other than the PD source and the bias voltage is provided by a 30 V source.

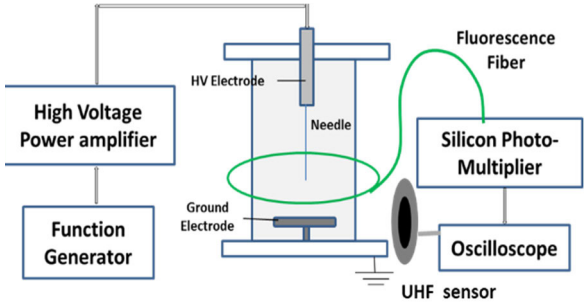

FIGURE 2. Experimental setup used for corona inception studies of nanofluids.

PD measurements were also made using non-directional broadband UHF Sensor with a bandwidth of 3 GHz [18], placed at a distance of 20 cm from the test cell. The incipient discharges detected by UHF Sensor and fluorescent fiber technique were then fed to a digital storage oscilloscope, with bandwidth of 3.5 GHz, sample-rate of 40 GSa/s, and 50 Ω input impedance. Measurements were made under both AC and DC voltages, using both UHF and fluorescence techniques for detection. Each presented CIV value is based on an average of 30 observations, with each observation being the voltage applied at the time when to the first discharge was detected by the UHF sensor and fluorescent fiber and the standard deviation in the measured values was found to be less than ±3%.

C. DIELECTRIC RESPONSE MEASUREMENT

The dielectric response was measured with the OMICRON-DIRANA instrument, which creates a sinusoidal signal at the required frequency. As per IEC 60247 standard, the oil test cell was connected to a DIRANA dielectric response analyzer using three electrodes: voltage, measuring and guard electrode. The test cell was equipped with a heating system that allowed for a maximum temperature of roughly 110°C and temperature equilibrium was maintained throughout the measuring period as the samples were heated from 30°C to 90°C.

D. FLOW ELECTRIFICATION STUDIES

A spinning disc apparatus was used to test streaming electrification of the fluid, with the cellulose material covering both sides of the disc as shown in Fig. 3. In this experiment, an aluminium disc with a diameter of 40 mm and a thickness of 6 mm was used. The cylindrical fluid-holding jar was built of aluminium with 85 mm in diameter and 100 mm in height. A motor with a speed regulator controlled the rotation of the disc between 0 and 600 rpm. While testing the effect of temperature on the charging current with varying disc velocities, a digital thermometer was inserted in the circulating oil to continuously monitor the oil temperature. The spinning disc system and its motor configuration were enclosed in a Faraday cage to reduce stray current, and the electrification current was measured using a Keithley picoammeter connected between the vessel and the ground.

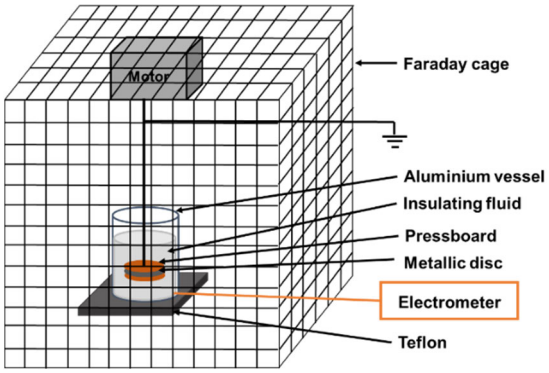

FIGURE 3. Flow electrification using spinning disc system.

E. RHEOLOGICAL STUDIES

Horiba SZ-100 nano partica instrument has been used to do zeta potential analysis where the stability of varying concentrations of SiO_2 nanoparticles in the synthetic ester fluid is studied with different surfactant. The fluorescence was measured using a Horiba aqualog spectrofluorometer with a 150 W xenon lamp. Excitation emission matrix (EEM) spectra were obtained at intervals of 15 nm in the wavelength range 250-700 nm, and emission wavelength range 350-800 nm at intervals of 1.1 nm. Rheological testing was done with a modular compact rheometer (Anton Paar, MCR 102) with a cone-plate geometry (CP 40). To achieve equilibrium, the samples were kept under high vacuum for 10 minutes before starting the experiment. Before any measurement, the gap spacing between the cone and plate was adjusted to 0.080 mm, which was maintained throughout the measurement period. The temperature on the plate was monitored using a P-PTD200/AIR Plate Peltier temperature device throughout the experiment.

III. RESULTS AND DISCUSSIONS

A. ZETA POTENTIAL ANALYSIS

Fig. 4 shows the zeta potential measurement for different concentration of silica and surfactant in the base fluids where

the absolute value indicated is based on the average of five measurements. Initially, the silica concentration in synthetic ester fluid (Sample B) is optimized where the specimen with 50 mg/L shows a relatively higher stability. In addition, the different surfactant concentrations of CTAB, Oleic acid and Span-80 were varied to the optimized level of SiO_2 nanofiller observed from Sample B. The suspended nanoparticles on the synthetic ester fluids can possess a higher positive or negative zeta potential if they retard the formation of agglomeration with a higher repulsive force. From the present work, the zeta potential value was found to increase marginally on the synthetic ester fluid containing surfactant compared to its influence without surfactant. On comparing the effect of different surfactants on the stability, the addition of CTAB was seen to result in a higher positive zeta potential. Also, a negative zeta potential was seen on the addition of Oleic acid and Span 80, which could be due to its higher pH value compared to CTAB surfactant [19], with a higher negative zeta potential observed on the nanofluids containing Span 80 as a surfactant. The higher solubility of Span 80 in base ester fluid could have occurred due to its hydrophilic feature of the 3-OH group and 18 carbon molecules whereas oleic acid containing the same number of carbon molecules with fewer OH groups, results in weaker bonds, making it less stable [20].

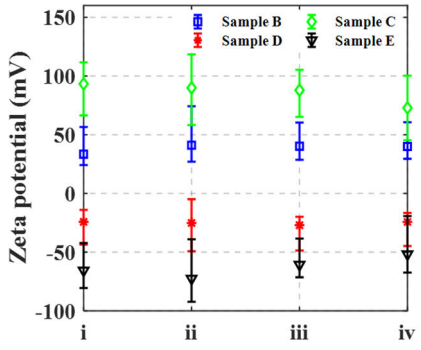

FIGURE 4. Zeta potential measurement of SiO_2 nanoparticle with and without surfactants. Sample B: (i) 25 mg/L, (ii) 50 mg/L, (iii) 75 mg/L, (iv) 100 mg/L; Sample C: (i) 0.25 mg/L, (ii) 0.5 mg/L, (iii) 0.75 mg/L, (iv) 1 mg/L; Sample D: (i) 25 μl/L, (ii) 50μl/L, (iii) 75 μl/L, (iv) 100 μl/L; Sample E: (i) 25 μl/L, (ii) 50 μl/L, (iii) 75 μl/L, (iv) 100 μl/L.

B. CORONA INCEPTION VOLTAGE

Fig. 5 shows the measured corona inception voltage (CIV) of synthetic ester based nanofluids with increasing amounts of SiO_2 and different surfactants (CTAB, Oleic acid, Span 80). Fig. 5a shows the CIV for samples of various SiO_2 concentrations (mg/L) in the synthetic ester fluid. The addition of silica nanoparticles resulted in a larger inception voltage when compared to base ester fluid. The CIV values showed a peak at 50 mg/L, gradually decreasing for higher concentrations. The dipole-dipole interactions between the silica nanoparticles govern the agglomeration process and could be the reason for the reduced inception voltage [21].

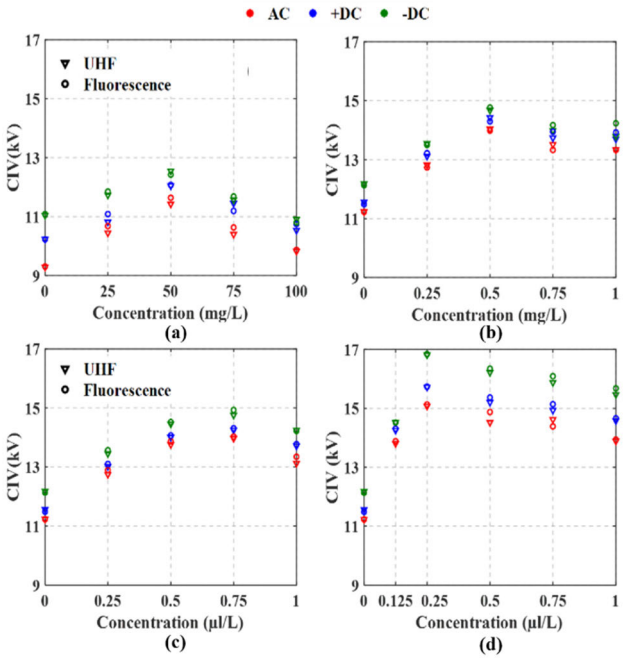

FIGURE 5. Variation in the corona inception voltage of (a) synthetic ester fluid with different SiO_2 nanoparticle concentrations, (b) synthetic ester fluid with 50 mg/L concentration of SiO_2 and different CTAB concentrations, (c) synthetic ester fluid with 50 mg/L concentration of SiO_2 and different oleic acid concentrations and (d) synthetic ester fluid with 50 mg/L concentration of SiO_2 and different Span 80 concentrations.

Further, at higher concentrations (greater than 50 mg/L), it could result in charge accumulation, thus causing the discharges to occur at lower voltages. The UHF approach identified incipient discharges at lower voltages in some cases, but the variation between this and the fluorescent fiber method was minimal. Thus, the fluorescent fiber can be used for corona discharge identification in transformers, if a suitable fiber is chosen based on the type of insulating fluid. Among the different voltage profiles, the −DC voltage gave a higher CIV compared to +DC and AC voltages. The charges due to applied electric field are trapped by the nanoparticles forming an opposing field at the needle electrode and thus requiring a higher voltage for the inception under −DC voltages. The effect of the different surfactant on the CIV was examined using the optimized concentration of SiO_2 (50 mg/L) and the concentrations of surfactants were varied as shown in Fig. 5b to Fig. 5d.

The CIV increases with the amount of different concentration of surfactants up to a certain limit and then decreases. At lower concentrations (0.5 mg/L of CTAB concentration, 0.75 μl/L of oleic acid and 0.25 μl/L concentration of Span-80), the addition of surfactant reduces the Van Der Waals attractive force between the nearby nanoparticles by encapsulating its surface area forming a stable nanofluid. But after a certain concentration, the surfactant fully covers the nanoparticles reducing the electrostatic repulsive force causing the agglomeration [21]. Sample E had a higher CIV compared to other sample under AC and DC voltages, with

about 62.5% and 52.2% increment respectively. The hydroxyl groups present in the Span 80 surfactant effectively bind to silica surfaces, resulting in better stability and improved inception voltage.

1) UHF AND FLUORESCENCE SIGNAL ANALYSIS

Fig. 6 and Fig. 7 show the typical fluorescence and UHF signals captured during the corona discharges, along with their frequency spectra. The fluorescent signal generated at the photomultiplier output was similar to a double exponent pulse and the energy content of the fluorescent signal ranges from 0 to 20 MHz. The UHF sensor's frequency content is observed from 300 MHz to 1 GHz with the dominant frequency at 0.9 GHz. UHF being a resonant sensor provides excellent stability and resolution of the output signal in frequency domain and are immune to fluctuations.

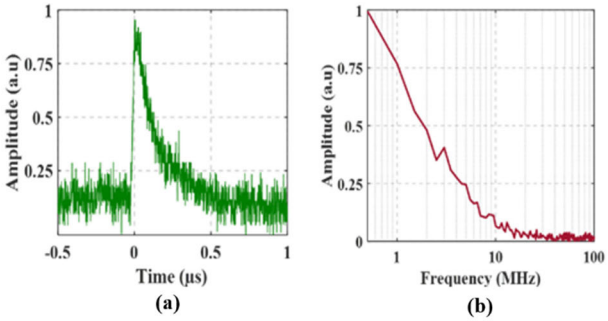

FIGURE 6. (a) Typical fluorescence signal under corona discharge and (b) fast fourier transform.

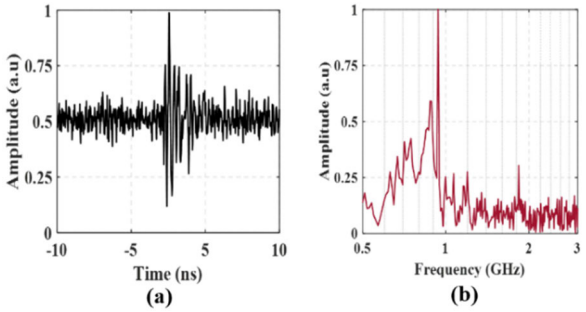

FIGURE 7. (a) Typical UHF signal under corona discharge and (b) fast fourier transform.

The signal captured using UHF sensor and fluorescent fiber can be related to corona discharge activity using parameters that are shown in Table 2. The rise time (t_r) of the signal involves 10% to 90% of the rising peak and the pulse width (t_{pw}) is the elapsed time between the leading (5%) and trailing (5%) edges of a signal. It is evident that rise time and pulse width of the signal increases with the addition of fillers and surfactant. This could be due to the requirement of higher energy to cause inception discharges in the medium, confirming the results of corona inception voltage.

TABLE 2. Signal parameters evaluated from UHF and fluorescence fiber.

Sample	UHF			Fluorescence		
	V_{pp} (V)	t_r (ns)	t_{pw} (ns)	V_p (mV)	t_r (ns)	t_{pw} (ns)
A	0.38	1.03	1.72	8.36	18.32	178.9
B	0.42	1.12	1.79	12.69	20.56	193.6
C	0.49	1.25	1.90	15.8	21.22	200.2
D	0.5	1.15	2.12	47.7	21.45	210.6
E	0.47	1.12	1.86	33.6	19.13	205.1

C. RHEOLOGY OF NANOFLUIDS

The rheological behavior of synthetic ester-based nanofluids with different surfactant have been understood through the relation exerted between the shear stress and shear rate as shown in Fig. 8a. The equation that relates these quantities for a fluid with Newtonian behavior is given by

$$\tau = \mu\gamma \tag{1}$$

where τ is the shear stress exerted on the fluid, γ is the shear rate and μ is the coefficient of viscosity. Both synthetic ester (Sample A) and its nanofluids (Sample B to E) obey Newton's law of viscosity where a linear variation of shear stress is observed with respect to shear rate. Also, there is not much variation in the shear stress exhibited on the addition of SiO_2 nanoparticles to the synthetic ester fluid and with impact of different surfactants. The fluid viscosity determines the resistance to shear and its flow conditions where a higher viscosity denotes more flow resistance. The viscosity was found to be independent of its shear rate (Fig. 8b) confirming the Newtonian behavior exhibited by both synthetic ester and its nanofluids. The magnitude of viscosity was higher for nanofluids (D > E > C > B) because of the shear thinning effect by colloidal suspension on the base fluid that interrupts the Brownian motion [22]. The shear rate was then maintained at 100 s^{-1} and its viscosity measurements were done with respect to temperature as shown in Fig. 9.

The viscosity followed an exponential relation with temperature as shown in Equation 2.

$$\nu(T) = \nu_0 e^{-\alpha T} \tag{2}$$

where $\nu(T)$ is the dynamic viscosity expressed a function of temperature, ν_0 is the initial viscosity (30°C), α is the decay rate and T is the temperature.

The decay rate associated with the viscosity parameter was higher for Sample A followed by Sample B, indicating its better flow characteristics compared to nanofluids with surfactant (Sample C to E). At ambient temperature conditions (30°C), a slight change has been exhibited between base synthetic ester (Sample A) and nanofluids (Sample B to E). Nevertheless, the viscosity of all samples got overlapped at a temperature greater than 40°C without much change exhibited at higher temperature. The combined effect of the non-Newtonian behavior of the fluids, as well

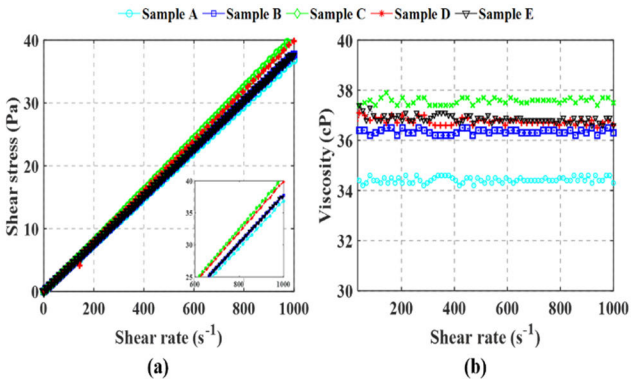

FIGURE 8. (a) Shear stress variation with shear rate and (b) Viscosity with shear rate.

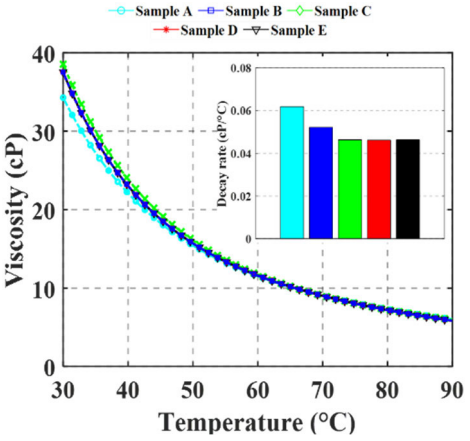

FIGURE 9. Variation of viscosity with temperature.

TABLE 3. Activation energy involved with flow conditions.

Sample	A	B	C	D	E
Activation Energy (kJ/mol)	20.55	20.60	17.32	14.13	17.62

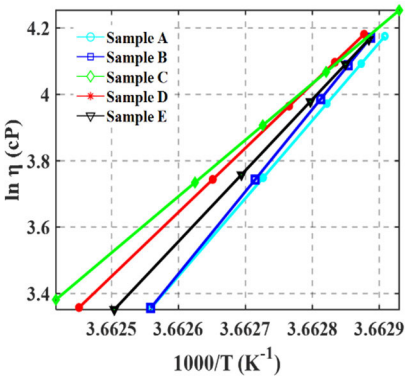

FIGURE 10. Arrhenius plot for the viscosity of synthetic ester-based silica nanofluids.

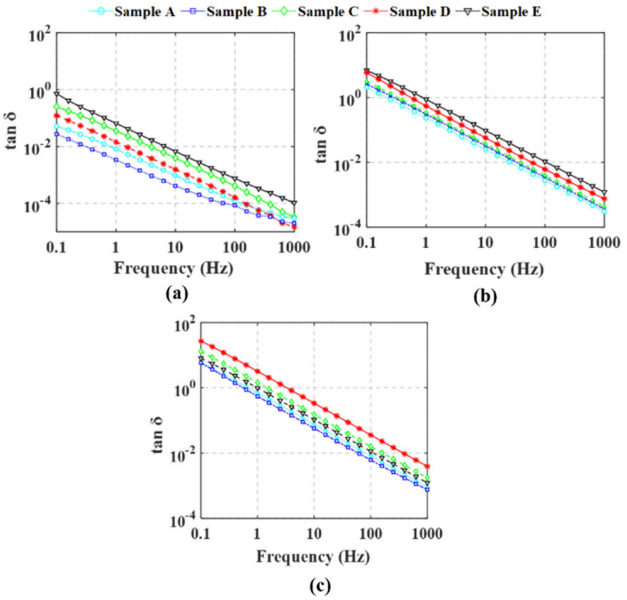

FIGURE 11. Variation of dissipation factor with frequency at (a) 30°C, (b) 60°C and (c) 90°C.

as a change in chemical composition that occurred at high temperatures, could be the reason behind the above trend in the viscosity [22].

Fig. 10 shows the Arrhenius plot evaluated from the experimental results of viscosity measurements with temperature. The viscosity followed an Arrhenius relation and the activation energy evaluated based on the slope is indicated in Table 3. The higher activation energy implies that more energy is required to dissociate the molecules present in the fluid and it also prevents the fast rise in the ionic mobility with increase in temperature [23]. The activation energy related to flow conditions followed the trend A > B > E > C > D, thus confirming the rheological properties with the stability of nanofluids.

D. DIELECTRIC RESPONSE SPECTROSCOPY

The OMICRON-DIRANA unit was used to explore the dielectric properties of the synthetic ester-based nanofluids for all samples (A to E) with enhanced performance characteristics (Fig. 5), and the findings are reported in Table 4 for measurements performed at 50 Hz. The lower dielectric constant at higher temperatures could be due to the weaker interaction between molecules, as well as a fall in the fluid's viscosity. At higher temperatures, the increase in kinetic energy causes Brownian motion of nanoparticles, which results in a reduction in dipole orientation and a decrease in permittivity [16].

The bulk polarizability of the nanoparticles in the base fluid determines the dielectric constant where the permittivity of samples B and C decreases slightly when the temperature rises, which could be due to the interfacial zone between the base fluid and nanoparticles. The nanoparticles attract charges on their surface when an external field is applied, creating a similar behavior as that of polar molecules and resulting in the orientational polarization. In addition, the effective

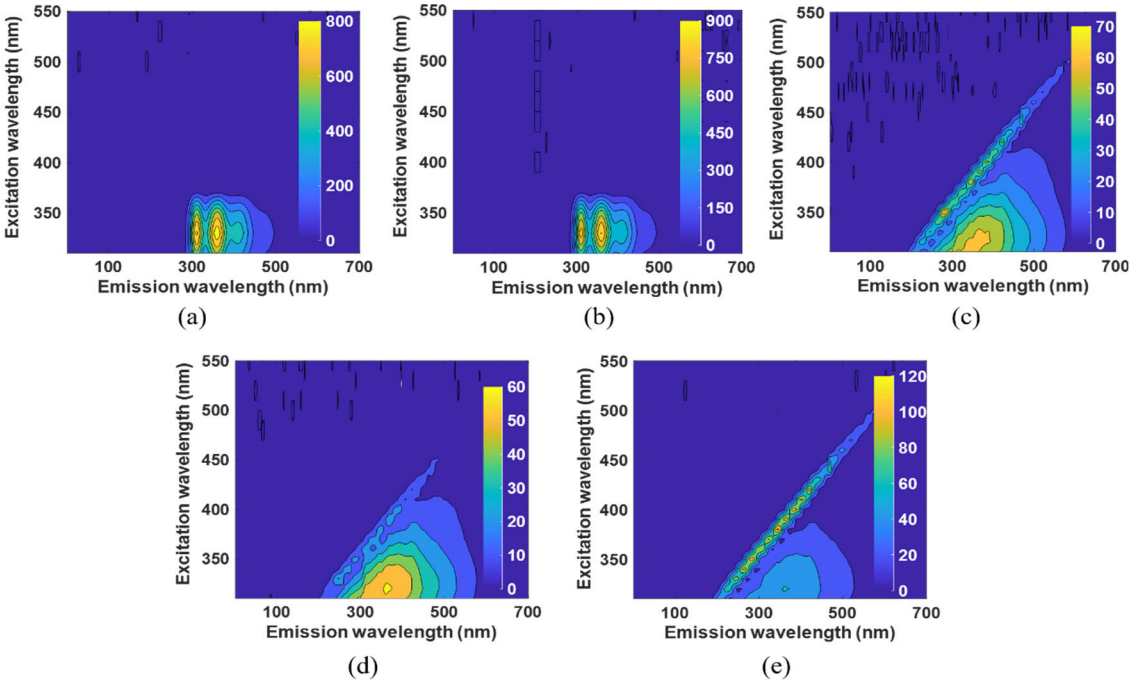

FIGURE 12. EEM Spectra of (a) Sample A, (b) Sample B, (c) Sample C, (d) Sample D, (e) Sample E.

TABLE 4. Activation energy involved with flow conditions permittivity and dissipation factor at power frequency.

Sample	30° C		90° C	
	ε_r	tan δ ($\times 10^{-3}$)	ε_r	tan δ ($\times 10^{-3}$)
A	3.212	1.685	2.901	10.2
B	3.22	0.912	2.902	9.57
C	3.235	5.75	2.923	17.5
D	3.242	10.253	3.025	56.12
E	3.233	2.345	3.056	24.33

polarizability of the nanofluid is aided by the inner polarization of nanoparticles, resulting in an increase in the permittivity [24]. Table 4 also reveals a temperature-dependent rise in the loss tangent, which could be attributed to larger relaxation loss at higher temperatures. As shown in Fig. 11, the variation in tan δ of ester and its nanofluids was examined over a wider frequency range (0.1 Hz to 1 kHz). The interfacial polarization dominates mostly at lower frequencies, resulting in charge generation at the interface between nanoparticles and dipole molecules of the base ester fluid, whereas tan δ decreases with frequency at higher range. Sample A observed the lowest loss factor compared to other samples (B to E) throughout its wide frequency range and temperature. The nanofluid containing Span 80 as surfactant (Sample E) showed a higher tan δ at 30°C and 90°C, which could be related to higher ionic mobility arising from the hydroxyl groups present in its molecular structure. The oleic acid based nanofluid (Sample D) observed lowest loss tangent at ambient temperature conditions whereas an opposite trend was seen at higher temperature (90°C) indicating its higher diffusion of ionic charges and lower stability. The CTAB surfactant (Sample C) although observed a higher loss tangent at lower temperature maintained its region to be in the same magnitude indicating its better stability even at higher temperatures.

E. FLUORESCENCE SPECTROSCOPY OF NANOFLUIDS

Fig. 12 shows the excitation emission matrix (EEM) of synthetic ester-based SiO_2 nanofluids and colour scale indicates the intensity of the fluorophore. The emission and excitation maxima of all the samples was in the range of 350-400 nm and no significant shift variation in the wavelengths was observed on the addition of silica nanoparticles and surfactants to the ester fluid. The molecules present in the insulating fluid are responsible for fluorescence, where a marginal reduction in the intensity has taken place upon the addition of surfactants (Sample C to Sample E) compared to Sample A and Sample B. The unsaturated fatty acids present in the ester fluid acts a primary source for the fluorescence behavior which gets altered upon the addition of surfactant and hence indicating a reduction in intensity. On examining the EEM spectra of ester based nanofluids, the fluorescent fiber used for detecting the corona discharge activity (Fig. 5) could be chosen and it can also assess the quality of fluid inside the real time power transformers.

F. ELECTROSTATIC CHARGING TENDENCY OF NANOFLUIDS

The streaming current of ester-based nanofluids measured under different rotational speed and temperatures is shown in Fig. 13. It was noticed that as the disc velocity increased, the streaming current increased too. This could be due to the rise in frictional force exerted between the disc and the insulating fluid, as well as the change in Debye length with increase in the rotational speed [25]. At lower disc velocities (<300 rpm), there was not much variation in the current magnitude observed for both ester and its nanofluids. A significant change got exhibited only at higher disc velocities due to the higher exchange of ions between the electrical double layer formed at the pressboard/fluid interface. Also, the effect of temperature further increases the charging current which could be related to the reduction in the kinematic viscosity and increase in the mobility of ions. On comparing the effect of different samples, Sample A and Sample B gave a lower current, which fits with the lower density of charge carriers present in these fluids, whereas Sample C showed a larger current magnitude of about five times as that of Sample A.

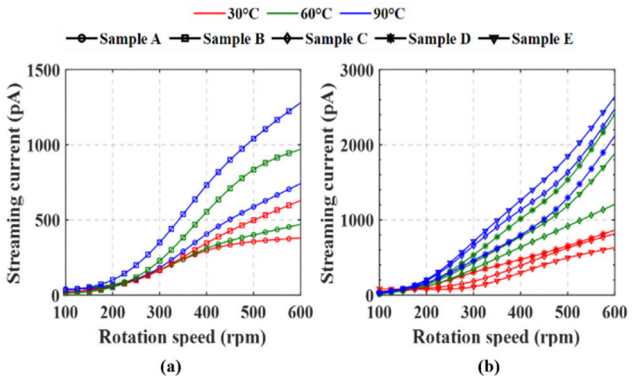

FIGURE 13. Streaming current of ester based nanofluids at different temperatures and rotational velocity for (a) Sample A and Sample B, (b) Sample C to Sample E.

The cationic surfactant (Sample C) interaction with the pressboard material causes more negative charges to be developed in the compact layer causing an equal number of positive charges to be diffused into the fluid. The non-ionic structure of Span 80 (Sample E) gave the lowest current at 30°C among all the nanofluids containing surfactant, but at higher temperature (90°C), the dissociation of hydroxyl groups takes place resulting in higher current with ester fluid containing Span 80 as a surfactant.

IV. CONCLUSION

- The stability of synthetic ester based nanofluids was analyzed using different surfactant and it is high with the addition of Span 80 showing a negative zeta potential because of its higher pH value compared to CTAB surfactant. The results were in accordance with the corona inception voltage showing better properties with Span 80 compared to other surfactants.
- The corona inception voltage measured by UHF technique and by fluorescent fiber technique are nearly the same. Hence, if the fluorescent fibres are suitably placed, they can be used as a condition monitoring of corona discharges inside transformers. The parameters such as pulse width and rise time obtained from fluorescence and UHF signal was very much lower for synthetic ester compared to its nanofluids.
- The rheological aspects of the nanofluids got reduced slightly with the addition of surfactants indicating a resistance to its flow conditions and no significant variation was observed in the viscosity parameter with shear stress indicating its Newtonian behavior even after the addition of surfactants.
- The dielectric studies show that the permittivity of nano ester fluid does not change greatly when the surfactant is added but a slight change is observed in the loss tangent measured at different temperatures, with CTAB providing a stable dielectric property compared to oleic acid and Span 80.
- The excitation emission matrix of ester nanofluids did not show any shift in its wavelength, but a significant change was observed in the fluorescence intensity.
- The streaming current of nanofluids was observed to be higher with the addition of surfactant. Considering the evaluation of different temperatures, the magnitude of current was higher for the ionic surfactant (CTAB) compared to non-ionic surfactant (Span 80).

The investigation of electro-rheological and spectroscopic studies of different surfactants towards silica based synthetic ester fluids have been experimented in the current work, and further, thermal conductivity of nanofluid can also depend on the stability which has been planned as a future scope of the present research work.

REFERENCES

[1] I. Fernández, A. Ortiz, F. Delgado, C. Renedo, and S. Pérez, "Comparative evaluation of alternative fluids for power transformers," *Electr. Power Syst. Res.*, vol. 98, pp. 58–69, May 2013.

[2] P. Rozga, A. Beroual, P. Przybylek, M. Jaroszewski, and K. Strzelecki, "A review on synthetic ester liquids for transformer applications," *Energies*, vol. 13, no. 23, p. 6429, Dec. 2020.

[3] W. Yu and H. Xie, "A review on nanofluids: Preparation, stability mechanisms, and applications," *J. Nanomater.*, vol. 2012, pp. 1–17, Jul. 2012.

[4] S. A. Khan, A. A. Khan, and M. Tariq, "Measurement of Tan-delta and DC resistivity of synthetic ester based oil filled with Fe_2O_3, TiO_2 and Al_2O_3 nanoparticles," *Smart Sci.*, vol. 9, no. 3, pp. 216–225, 2021.

[5] Z. Nadolny and G. Dombek, "Electro-insulating nanofluids based on synthetic ester and TiO_2 or C_{60} nanoparticles in power transformer," *Energies*, vol. 11, no. 8, p. 1953, Jul. 2018.

[6] Q. Khan, V. Singh, F. Ahmad, and A. A. Khan, "Dielectric performance of magnetic nanoparticles-based ester oil," *IET Nanodielectr.*, vol. 4, no. 2, pp. 45–52, Jun. 2021.

[7] U. Khaled and A. Beroual, "AC dielectric strength of synthetic ester-based Fe_3O_4, Al_2O_3 and SiO_2 nanofluids—Conformity with normal and Weibull distributions," *IEEE Trans. Dielectr. Electr. Insul.*, vol. 26, no. 2, pp. 625–633, Apr. 2019.

[8] G. D. P. Mahidhar, R. Sarathi, N. Taylor, and H. Edin, "Dielectric properties of silica based synthetic ester nanofluid," *IEEE Trans. Dielectr. Electr. Insul.*, vol. 27, no. 5, pp. 1508–1515, Oct. 2020.

[9] D. Dey, P. Kumar, and S. Samantaray, "A review of nanofluid preparation, stability, and thermo-physical properties," *Heat Transf.-Asian Res.*, vol. 46, no. 8, pp. 1413–1442, Dec. 2017.
[10] X.-J. Wang, X. Li, and S. Yang, "Influence of pH and SDBS on the stability and thermal conductivity of nanofluids," *Energy Fuels*, vol. 23, no. 5, pp. 2684–2689, May 2009.
[11] S. N. Suhaimi, A. R. A. Rahman, M. F. M. Din, M. Z. Hassan, M. T. Ishak, and M. T. B. Jusoh, "A review on oil-based nanofluid as next-generation insulation for transformer application," *J. Nanomater.*, vol. 2020, pp. 1–17, Feb. 2020.
[12] W. T. Urmi, M. M. Rahman, K. Kadirgama, D. Ramasamy, and M. A. Maleque, "An overview on synthesis, stability, opportunities and challenges of nanofluids," *Mater. Today, Proc.*, vol. 41, pp. 30–37, Jan. 2021.
[13] N. Petkova, P. Nakov, and V. Mladenov, "Real time monitoring of incipient faults in power transformer," in *Electricity Distribution*. Berlin, Germany: Springer, 2016, pp. 221–240.
[14] M. R. Hussain, S. S. Refaat, and H. Abu-Rub, "Overview and partial discharge analysis of power transformers: A literature review," *IEEE Access*, vol. 9, pp. 64587–64605, 2021.
[15] H. Chai, B. T. Phung, and S. Mitchell, "Application of UHF sensors in power system equipment for partial discharge detection: A review," *Sensors*, vol. 19, no. 5, p. 1029, Feb. 2019.
[16] A. J. Amalanathan, R. Sarathi, N. Harid, and H. Griffiths, "Investigation on flow electrification of ester-based TiO_2 nanofluids," *IEEE Trans. Dielectr. Electr. Insul.*, vol. 27, no. 5, pp. 1492–1500, Oct. 2020.
[17] M. S. Vihacencu, P. V. Notingher, T. Paillat, and S. Jarny, "Flow electrification phenomenon for Newtonian and non-Newtonian liquids: Influence of liquid conductivity, viscosity and shear stress," *IEEE Trans. Dielectr. Electr. Insul.*, vol. 21, no. 2, pp. 693–703, Apr. 2014.
[18] M. D. Judd, Y. Li, and I. B. B. Hunter, "Partial discharge monitoring of power transformers using UHF sensors. Part I: Sensors and signal interpretation," *IEEE Elect. Insul. Mag.*, vol. 21, no. 2, pp. 5–14, Mar./Apr. 2005.
[19] A. I. Khan and A. V. Arasu, "A review of influence of nanoparticle synthesis and geometrical parameters on thermophysical properties and stability of nanofluids," *Thermal Sci. Eng. Prog.*, vol. 11, pp. 334–364, Jun. 2019.
[20] M. Akbari, M. Yavari, N. Nemati, J. B. Darband, H. Molavi, and M. Asefi, "An investigation on stability, electrical and thermal characteristics of transformer insulting oil nanofluids," *Int. J. Eng.*, vol. 29, no. 10, pp. 1332–1340, 2016.
[21] G. D. P. Mahidhar, R. Sarathi, N. Taylor, and H. Edin, "Study on performance of silica nanoparticle dispersed synthetic ester oil under AC and DC voltages," *IEEE Trans. Dielectr. Electr. Insul.*, vol. 25, no. 5, pp. 1958–1966, Oct. 2018.
[22] K. Anoop, R. Sadr, M. Al-Jubouri, and M. Amani, "Rheology of mineral oil-SiO_2 nanofluids at high pressure and high temperatures," *Int. J. Thermal Sci.*, vol. 77, pp. 108–115, Mar. 2014.
[23] S. O. Oparanti, A. A. Khaleed, and A. A. Abdelmalik, "Nanofluid from palm kernel oil for high voltage insulation," *Mater. Chem. Phys.*, vol. 259, Feb. 2021, Art. no. 123961.
[24] N. Baruah, M. Maharana, S. S. Dey, and S. K. Nayak, "Nanoparticle polarization effect on the permittivity of the dielectric liquid," in *Proc. IEEE 20th Int. Conf. Dielectr. Liq. (ICDL)*, Jun. 2019, pp. 1–4.
[25] M. Talhi, I. Fofana, and S. Flazi, "Comparative study of the electrostatic charging tendency between synthetic ester and mineral oil," *IEEE Trans. Dielectr. Electr. Insul.*, vol. 20, no. 5, pp. 1598–1606, Oct. 2013.

S. K. AMIZHTAN is currently a Research Scholar with the Department of Electrical Engineering, IIT Madras, Chennai, India. His research interests include condition monitoring and characterization of nanofluid-based transformer insulation.

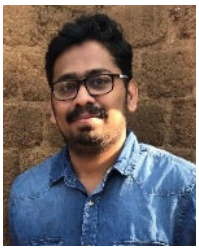

A. J. AMALANATHAN is currently a Research Scholar with the Department of Electrical Engineering, IIT Madras, Chennai, India. His research interests include condition monitoring of ester and its nanofluids for power transformers.

R. SARATHI (Senior Member, IEEE) is currently a Professor and the Head of the High Voltage Laboratory, Department of Electrical Engineering, IIT Madras, Chennai, India. His research interests include condition monitoring of power apparatus and nanomaterials.

BALAJI SRINIVASAN (Member, IEEE) is currently a Professor with the Department of Electrical Engineering, IIT Madras, Chennai, India. His research interests include development of active and passive optical components/subsystems for distributed fiber optic sensors and fiber lasers.

RAMESH L. GARDAS is currently a Professor with the Department of Chemistry, IIT Madras, Chennai, India. His research interests include ionic liquids, chemical thermodynamics, fluid phase equilibria, group contribution methods, and structure-property correlations.

HANS EDIN (Member, IEEE) was born in Sandviken, Sweden, in April 1971. He received the M.Sc. and Ph.D. degrees in electrical engineering from the Royal Institute of Technology (KTH), Stockholm, Sweden, in 1995 and 2001, respectively. He is currently a Professor with the Royal Institute of Technology. He is involved in research concerning development of insulation diagnostic methods for high voltage equipment. In particular, partial discharge analysis and dielectric spectroscopy.

NATHANIEL TAYLOR (Member, IEEE) was born in Oxford, U.K., in 1978. He received the M.Eng. degree in electrical and electronic engineering from the Imperial College London, in 2001, and the Ph.D. degree from the KTH Royal Institute of Technology, in 2010, in the subject of high-voltage insulation. He is currently working as a Researcher with the School of Electrical Engineering, KTH, working on power-system component design and diagnostics.